

# Down-regulation of Risa Improves Podocyte Injury by Enhancing Autophagy in Diabetic Nephropathy

**Peipei Su**

Zhengzhou University First Affiliated Hospital

**Dongwei Liu** (✉ [liu-dongwei@zzu.edu.cn](mailto:liu-dongwei@zzu.edu.cn))

Zhengzhou University First Affiliated Hospital

**Sijie Zhou**

Zhengzhou University First Affiliated Hospital

**Hang Chen**

The Third People's Hospital of Zhengzhou

**Xianming Wu**

The Third People's Hospital of Zhengzhou

**Zhangsuo Liu**

Zhengzhou University First Affiliated Hospital

---

## Research

**Keywords:** Diabetic Nephropathy, LncRNA AK044604/Sirt1/GSK3 $\beta$ , Autophagy

**Posted Date:** November 16th, 2021

**DOI:** <https://doi.org/10.21203/rs.3.rs-989734/v1>

**License:**  This work is licensed under a Creative Commons Attribution 4.0 International License.

[Read Full License](#)

---

# Abstract

## Background

LncRNA AK044604 (Risa), Sirt1 and GSK3 $\beta$  are autophagy related genes that can play important roles in diabetic nephropathy (DN). In this study, we sought to explore the effect of Risa on Sirt1/GSK3 $\beta$ -induced podocyte injury.

## Methods

Transgenic db/db mice were fed and injected with Risa inhibition of adeno-associated virus by tail vein injection, as well as intraperitoneally injected with LiCl. Blood, urine, kidney tissue samples, and clinical data were collected at different time points. Immortalized mouse podocyte cells (MPCs) were cultured and treated with Risa inhibition of lentivirus, EX-527, and LiCl. MPCs were collected under different stimulations. The effects of Risa on podocyte autophagy were examined by qRT-PCR, Western blot analysis, transmission electron microscope, PAS staining, and immunofluorescence staining.

## Results

Risa and activated GSK3 $\beta$  were overexpressed, but Sirt1 decreased in Renal tissues of DN mice and high-glucose-treated MPCs and correlated with poor prognosis. Risa overexpression attenuated Sirt1-mediated downstream autophagy levels and aggravated the injury of podocytes by inhibiting the expression of Sirt1. In contrast, Risa inhibition enhanced Sirt1-induced autophagy and attenuated podocyte injury, but this effect could be abrogated by EX-527, suggesting that Risa overexpression aggravated podocyte injury by decreasing autophagy.

## Conclusions

Risa inhibits autophagy by regulating the Sirt1/GSK3 $\beta$  axis and thereby aggravates podocyte injury in DN. Risa may serve as a therapeutic target for the treatment of DN.

## Background

Diabetic nephropathy (DN) is a serious public health problem with an increasing incidence worldwide, which lacks effective treatment. Approximately 40% of patients with diabetes develop end-stage renal disease (ESRD) [1]. Therefore, it is urgent to find new therapeutic methods and targets.

Hyperglycemia-mediated alterations of extracellular and intracellular metabolism and nutrients, such as advanced glycation end products, increased protein kinase C activity, and abnormal polyol metabolism [2], intracellular stress associated with renal hypoxia [3], mitochondrial reactive oxygen species [4], endoplasmic reticulum stress [5], and nutrient depletion have been recognized as pathogenesis of DN. Autophagy is a highly conservative cellular process that degrades and recycles misfolded or dysfunctional proteins and damaged organelles to maintain cellular homeostasis via the lysosome

pathway [6]. Autophagy is regulated by nutrient state and intracellular stress, which are altered under diabetic conditions, and then the corresponding alterations of Sirt1, AMPK, and mTOR autophagy pathways potentially exacerbate organelle dysfunction and lead to DN [7]. High glucose and nutrient abnormalities under diabetic conditions increase intracellular stresses and inhibit autophagy by inhibiting Sirt1 and AMPK, and by activating mTOR, leading to the occurrence and progression of DN [8]. These findings indicate that hyperglycemia-induced alterations in autophagic activity are the key mechanism underlying diabetes-related podocyte injury.

Sirtuin type-1 (Sirt1) is a member of the silent information regulator 2 (Sir2)-like family of proteins [9]. Sirt1 is involved in many physiological processes, such as metabolism, mitochondrial homeostasis, cell proliferation, autophagy, and apoptosis [10]. Sirt1 is a positive regulator of autophagy [11]. Once activated, Sirt1 promotes autophagy by deacetylating relevant autophagy proteins, such as ATG5, ATG7, Beclin-1, LC3, and P62 [12]. In addition, Sirt1 can crosstalk with AMPK and mTOR pathways and regulate energy metabolism and prosurvival pathways including autophagy [13]. Low expression of Sirt1 has been found in podocyte injury during DN [13, 14]. Moreover, specific knockdown of Sirt1 in podocytes induced severe podocyte damage and increased proteinuria, whereas kidney damage was significantly alleviated after Sirt1 overexpression in diabetic mice [15, 16]. Therefore, the expression of Sirt1 in podocytes influence the occurrence and development of DN.

Glycogen synthase kinase3 $\beta$  (GSK3 $\beta$ ), a serine/threonine kinase and a key regulator of numerous cellular processes, ranging from glycogen metabolism to cell cycle regulation and proliferation [17]. GSK3 $\beta$  has complex and multitargeted biological effects, including multiple pathways such as insulin resistance, oxidative stress, autophagy, and apoptosis in podocyte injury of DN [17]. The expression of GSK3 $\beta$  increased in the high glucose environment of podocytes, and LiCl (GSK3 $\beta$  inhibitor) could alleviate podocyte injury induced by high glucose [18]. Increasing evidences have proved that the nutrient energy imbalance caused by abnormal glucose metabolism leads to excessive autophagy inhibition and GSK3 $\beta$  activation, GSK3 $\beta$  inhibition prevents ubiquitin proteome degradation of rapamycin (mTOR) mammalian targets, thereby enhancing autophagy [19, 20]. Therefore, GSK3 $\beta$  and autophagy play important roles in in podocyte injury and dysfunction of DN.

LncRNAs have recently been confirmed to have key roles in the pathobiological process of diabetic kidney disease (DKD), including diabetic tubular disease and diabetic glomerular diseases, such as podocytosis, endothelial dysfunction, mesangial lysis, and mesangial dilation. Many LncRNAs have been confirmed to be involved in podocyte damage in DN. For example, LncRNA TUG1 is related to the metabolic changes of podocytes in DN mice [21]. MALAT1 is dysregulated in DN and participates in high-glucose-induced podocyte injury through interaction with  $\beta$ -catenin in glomerular endothelial cells [22]. GM5524 can induce podocyte apoptosis and autophagy [23]; GM15645 can inhibit the podocyte apoptosis and autophagy of M1MALAT1 [23]. A transcription which is very close to Sirt1 has been found in the mouse genome. This transcript is identified as LncRNA AK044604, located in the 10qb4 region, and named as insulin sensitivity and autophagy regulator (Risa) [24]. Risa can regulate insulin sensitivity and

autophagy in vivo and in vitro. Down-regulation of Risa can improve insulin sensitivity by enhancing autophagy in ob/ob mice [24].

In this research, we found that Risa was strongly overexpressed in db/db mice renal tissues and high-glucose-induced MPCs, and then we predicted its targets (miRNAs) by bioinformatics methods and verified it in vitro and in vivo. The results revealed that Risa could reduce the repression of the downstream target gene via the Sirt1-mediated autophagy pathway and then promote the progression of DN. In short, our results showed that Risa might act as a pathogenic gene in DN progression and could be a potential biomarker for screening and treatment of DN.

## Materials And Methods

### Animal studies

db/db mice and healthy control db/m mice were housed and maintained under a 12-h light/12-h dark cycle, with ad libitum access to water and standard mouse chow at the First Affiliated Hospital of Zhengzhou University (Zhengzhou, Henan, China). Animals were maintained under specific pathogen-free conditions and received humane care according to the criteria outlined in the National Institutes of Health (NIH) Guide 21. The animal study was approved by the Institutional Animal Care and Use Committee of Zhengzhou University (2020-KY-273).

According to the manufacturer's instructions (Genechem Co., LTD., Shanghai, China), an adeno-associated virus (AAV) vector that interferes with Risa. Risa was amplified by PCR using specific primers (forward: 5'-TCTGGAGAGCCCAACCT-3', reverse: 5'-TCCTTCAA ACGCGAGAGAG-3'). qRT-PCR was used to detect the virus titer. Mice were divided into four groups: db/m, db/db, db/db+Risa-vehicle, and db/db+Risa-AAV. 10-weeks-old db/db mice were injected with Risa-AAV and the empty virus control group by tail vein injection under the red light vein imaging instrument. Blood, urine, kidney tissue, and clinical data (blood glucose, body weight, serum creatinine, and urinary albumin-creatinine ratio) were collected at the 6th, 10th, 14th, 18th and 22th weeks of age, while quantitative real-time polymerase chain reaction (qRT-PCR), Western blot analysis, transmission electron microscope (TEM), PAS and confocal immunofluorescence staining and analysis were used to observe the relevant indicators.

### Cell Culture and Transfection

The immortalized mouse podocyte cell (MPC) was donated by academician Liu Zhihong of Nanjing University School of Medicine (Nanjing, China). MPCs were immediately placed into a water bath at 37 °C with gentle shaking after the liquid nitrogen had evaporated. When completely melted, the cryopreservation-containing cells were transferred to a sterilized 5 mL centrifuge tube and centrifuged for 10 min at 1000 × g. After the supernatant was removed, the cells were resuspended in complete culture solution and inoculated in a culture dish with complete culture medium containing 45 mL of Royal Park Memorial Institute (RPMI)-1640 medium, 5 mL of fetal bovine serum (FBS), 50 μL of a mixture of penicillin/streptomycin at a ratio of 1:1000 and 1000 U γ-interferon (γ-IFN). The cells were evenly

distributed through gentle shaking and then placed in the culture incubator. The culture conditions were set at 33 °C with 5% CO<sub>2</sub> under saturated humidity. The medium was changed the next day, and cell growths were observed. When cell confluence reached 70–80%, the cells were subcultured at a ratio of 1:3. The cells that were cultured at 33 °C were inoculated into a fresh, precoated culture bottle with  $\gamma$ -IFN-free 1640 medium added. Then, the culture bottle was placed into an incubator at 37 °C with 5% CO<sub>2</sub>. Microscopically, the cells proliferated slowly, the cytoplasm extended to the periphery, and a large number of secondary protrusions emerged from the cell body. With 10–14 days of differentiation and maturation, the cells could be used in related experiments. Grouping was conducted as follows: i) NG (5.6 mM glucose); ii) HM (5.6 mM glucose + 44.4 mM mannitol); iii) HG (30 mM glucose); iv) HG + Lithium chloride (LiCl) (30 mM); v) HG+Risa-LV; vi) HG+Risa-vehicle; vii) HG+Risa-LV+ EX-527 (Sirt1 inhibitor). After 0-96 h, the podocytes were collected to be used for various assays. LiCl was purchased from Beijing DingGuo Changsheng Biotechnology (Beijing, China) and EX-527 was purchased from Beijing Bioss Biotechnology (Beijing, China).

Stable transfection of MPC cells with LncRNA AK044604 Lentivirus (Risa-LV) (Genechem, Shanghai, China) and empty vector (Risa-vehicle) were conducted referring to the instructions of the Reliable partner in gene function & drug target validation (Genechem, Shanghai, China).

### **RNA Extraction and qRT-PCR**

Tissue and cell total RNA were extracted using TRIZOL reagent (Thermo Fisher Scientific, Shanghai, China). RNA was used to perform reverse transcription using First Strand cDNA Synthesis Kit and polymerase chain reaction using SYBR Green qPCR kit (Thermo Fisher Scientific). Relative gene expression data were calculated using the comparative threshold cycle method with GAPDH or  $\beta$ -actin (Servicebio Co., LTD., Wuhan, China) as housekeeping genes. All assays were run in triplicate. The primers for each gene are as follows: Beclin-1, 5'-GAGTGG AATGA AATCAATGCTGC-3' and 5'-TTTCCACCTCTTCTTTGAACTGC-3'; LC3B, 5'-CCGTCCGAGAAGACCTTCAA-3' and 5'-TCTTGCGGCAG GAGAACCTA-3'; GAPDH, 5'-CCTCGTCCCGTAGACAAAATG-3' and 5'-TGAGGT CAA TGAAGGGGTC GT-3'.

### **Western Blot Assay**

Total protein lysates were extracted from mouse renal cortex tissue or cells using RIPA lysis buffer (Solarbio Co., LTD., Beijing, China). Protein samples were separated by 10–12% sodium dodecyl sulphate-polyacrylamide gel electrophoresis and transferred to polyvinylidene fluoride. After being blocked with 5% skim milk in phosphate-buffered saline with 0.1% Tween 20 for 1 h, the membranes were incubated with a primary antibody at 4°C overnight and then with a secondary antibody at room temperature for 1 h. High sig ECL Western blotting substrate development kit was used to develop the imprint. The relative gray intensity of each target protein expression band was quantitatively analyzed by Image J, and GAPDH was set as an internal reference. The ratio of each target protein to GAPDH was the relative expression level of the target protein. All measurements were repeated at least three times. Primary antibodies against SYSTM1/P62, Beclin-1, GSK3 $\beta$ , LC3B, Desmin, and WT-1 were purchased from Servicebio Biotechnology (Wuhan, China), GSK3 $\beta$  (phospho Ser9) was gained from Cell Signaling

Technology (Shanghai,China), Nephrin and NPHS2 were purchased from Abcam (Shanghai, China), Sirt1 and phospho Sirt1 (Ser 27) were obtained from Bioss Biotechnology (Beijing, China) , and GAPDH was acquired from Good Here (Hangzhou, China).

### **Transmission electron microscopy**

The kidney specimens were fixed in glutaraldehyde immediately after biopsy or nephrectomy. Ultrathin sections were cut with an ultramicrotome, stained with 2% uranyl acetate and lead citrate, and examined with a JEOL JEM-1400 Plus transmission electron microscope. Autophagosomes in podocytes were identified [7,8] under 5000× and 25,000× high-power field. Each tissue sample was examined; ten podocytes were randomly selected to count the number of autophagosomes and autophagolysosomes in podocytes. After counting, statistical analysis were performed by an experienced pathologist and nephrologist.

### **Renal histology**

Formalin-fixed and paraffin-embedded kidney tissues were prepared as 4µm sections and deparaffinized and hydrated. Sections were processed for periodic acid-Schiff staining. Slides were rinsed in distilled water after oxidizing in 0.5% periodic acid for 5 min, incubated in Schiff reagent for 15 min, washed in lukewarm tap water for 5 min, and counterstained in Mayer's hematoxylin.

### **Confocal immunofluorescence staining and analysis**

Kidney tissue sections or cells were fixed using cold methanol for 40 min and incubated overnight at 4 °C with primary antibodies. Secondary antibodies conjugated with Alexa Fluor® 488 or 594 were incubated at 25 °C for 1 h. Finally, sections were counterstained with Propidium Iodide and visualized by the Zeiss LSM 880 confocal microscope. Primary antibodies against SQSTM1/P62 and Nephrin were purchased from Servicebio Biotechnology (Wuhan,China), LC3B was obtained from Sigma-Aldrich (Shanghai, China), GSK3β (Phospho Ser9) was gained from Cell Signaling Technology (Shanghai, China), WT-1 was acquired from Santa Cruz Biotechnology (Shanghai, China), and phospho Sirt1 (Ser 27) was gained from Bioss Biotechnology (Beijing, China).

### **Statistical analyses**

Statistical analyses were performed using SPSS or Prism software. Data were expressed as means ± standard deviation (Unless otherwise stated). Continuous variables were compared using ANOVA and independent t-test. *P*-values < 0.05 in two-tailed tests were considered statistically significant in all analyses.

## **Results**

### **Effect of Risa Overexpression and Inhibition on High-Glucose-Induced Podocyte Injury**

High Glucose could stimulate the injury of podocytes. We initially determined Risa expression in DN mice or MPCs following different stimulations. qRT-PCR results showed that Risa expression in DN mice was significantly higher than healthy controls, but decreased after Risa-AAV treatment (Figure 1A). Similarly, the expression of Risa in HG group increased significantly compared with healthy control groups (NG, HM), but decreased after Risa-LV treatment (Figure 1B). qRT-PCR results confirmed the successful overexpression and inhibition of Risa in high-glucose-induced MPCs (Figures 1A,B). We then examined the effect of Risa overexpression and inhibition on podocyte injury. Western blot and immunofluorescence staining results supported that overexpressions of Risa in db/db mice group (Figures 1C,E) or high-glucose-treated MPC group (Figures 1D,F) had poor levels of podocyte expression. However, the levels of podocyte expression were increased markedly after Risa-AAV or Risa-LV treatment (Figures 1C-F). Moreover, TEM results showed that thickness of the glomerular basement membrane (GBM) were significantly increased, and the number of foot processes reduced in db/db mice, but GBM thicknesses were decreased after Risa-AAV therapy, as well as foot processes repaired (Figures 1G,H). Again, PAS staining results revealed that the morphology of kidney was disordered, such as matrix hyperplasia and vanishment of the cyst cavity markedly improved after Risa-AAV treatment (Figure 1G). Finally, we observed the changes of clinical indexes in mice and found that the blood glucose, body weight, urinary ACR, and blood creatinine of db/db mice were significantly higher than db/m mice (Figures 1I-L), whereas body weight, urinary ACR and blood creatinine were significantly decreased except blood glucose after Risa-AAV treatment in db/db mice compared with db/db control groups (Figures 1I-L). Of note, high-glucose-induced podocyte injury and renal function damage were counteracted by Risa inhibition but aggravated by Risa overexpression (Figures 1A-L). Taken together, Risa blocking abrogated the synergist effects of Risa overexpression on podocyte injury and renal function damage.

### **Effect of Risa Overexpression and Inhibition on High-Glucose-Induced Autophagy Damage**

Attenuation of podocyte autophagy has been shown to exert a podocyte- destructive effect in DN [25, 26]. Thus, we sought to determine whether autophagy attenuation is involved in the destructive effect of Risa in podocytes. Firstly, MPCs autophagy were assessed by immunofluorescence of LC3B (Figure 2A) and western blot analysis of autophagy-related markers (LC3B, Beclin-1, P62 and GSK3 $\beta$ ) (Figures 2B-D) in different observation times and in different stimulations. The expressions of LC3II (Figure 2B), phosphorylation of GSK3 $\beta$  (Figure 2D), and podocyte protective proteins (WT-1 and NPHS2) (Figure 2E), as well as the ratio of LC3II/I (Figure 2C) decreased with the lapse of time of high glucose stimulation, and decreased significantly after 24 hours, whereas an opposite trend was observed for P62 and Desmin (Figure 2B,E). Therefore, podocyte autophagy decreased gradually with the prolongation of high glucose stimulation. We then examined the effect of Risa overexpression and inhibition on podocyte autophagy. qRT-PCR and western blot results showed that expressions of Beclin-1, LC3B (Figures 2F-I) and phosphorylated GSK3 $\beta$  (Figures 2R-S) in DN mice and high-glucose-mediated MPCs were significantly lower than healthy controls, but increased after Risa-AAV or Risa-LV treatment (Figures 2F-I). The trend of LC3B expression in immunofluorescence results was the same as qRT-PCR and western blot results in both DN mice or high glucose MPCs (Figures 2L,M). Besides, TEM results revealed that the numbers of autophagosomes in DN mice and high glucose MPCs were lower than healthy control groups, but

increased after Risa-AAV or Risa-LV therapy (Figures 2N-Q). Diabetes environment or high glucose enhanced the inhibition of protein levels of LC3B, Beclin-1, phosphorylated GSK3 $\beta$ , the ratio of LC3II/LC3I (Figures 2J,K), and number of autophagosomes (Figures 2N-Q), while an opposite trend was observed for P62 (Figures 2H,I). Thus, the damage of podocyte autophagy by high glucose was counteracted by Risa inhibition but aggravated by Risa overexpression. We also found that Risa inhibiting abrogated the synergist effects of Risa overexpression on autophagy damage.

### **Risa Overexpression Aggravated the High-Glucose-Induced podocyte Injury by Reducing Autophagy**

The above researching conclusions indicated that Risa expression increased, as well as podocyte and autophagy damage increased in high glucose, and Risa inhibition could improve podocyte and autophagy damage. Thus, the changes of Risa, podocyte and autophagy damage showed consistent changes. To verify the autophagy pathway, podocyte autophagy was observed by treatment with Licl (an activator of autophagy, also an inhibitor of GSK3 $\beta$ ) in DN mice or high glucose MPCs. Western blot and immunofluorescence results showed that treatment with Licl had increased the expressions of LC3B and NPHS2 in db/db mice (Figures 4A,E,G) and high glucose MPCs (Figures 4B,F,H), as well as the ratio of LC3II/I (Figure 4C,D). Of note, Licl treatment abrogated the autophagy injury effect of Risa overexpression in DN mice and high glucose MPCs, reversing the Risa overexpression-mediated injury of podocyte autophagy. These results implied that Risa overexpression aggravated the high-glucose-induced podocyte injury by reducing autophagy.

### **Risa Suppressed Autophagy and Aggravated Podocyte Injury Via Sirt1-mediated Autophagy Axis**

To explore the relationship between Risa and high-glucose-induced podocyte autophagy pathway, our bioinformatics analysis revealed that there were putative binding sites between Risa, GSK3 $\beta$  and miRNAs (miR-6380, miR-706, miR-1195 and miR-3098-5p). We transfected miRNA mimics into HEK293T cells. The mmu-miR-6380/mmu-miR-706/mmu-miR-1195/mmu-miR-3098-5p significantly downregulated the expression of luciferase of m-AK044604-3UTR-WT (Supplemental Figure 1A-C). In contrast, there were no significant differences in luciferase activity cotransfected with mmu-miRNAs and m-GSK3 $\beta$ -3UTR-WT (Supplemental Figure 1D-H).

Risa is located close to Sirt1 and plays an important role in regulating insulin sensitivity and autophagy in vitro and in vivo [24]. Sirt1, an autophagy marker, interacts with components of the autophagy machinery [12, 27, 28, 29]. Diabetes-induced downregulation of Sirt1 leads to reducing autophagy and accelerating the pathogenesis of DN [30, 31, 32, 33]. Therefore, both Risa and Sirt1 have the function of regulating autophagy. We suppose that there are interactions between them in the process of DN, and crosstalks of Risa and autophagy might be a therapeutic target for preventing and treating DN. However, the precise molecular mechanisms are not fully understood. Thus, we speculated that Risa could bind to RNA or protein in a high glucose environment and relieve the levels of downstream (GSK3 $\beta$ , Beclin-1, and LC3B) autophagy by Sirt1, thereby leading to podocyte damage. Western blot and immunofluorescence results showed that Sirt1 inhibitor (EX-527) greatly decreased the phosphorylation of Sirt1 and GSK3 $\beta$  expressions in high-glucose-induced Risa inhibition MPCs (Figure 4A, D). Furthermore, the levels of

podocyte markers (NPHS2, WT-1, and Nephlin) significantly decreased by EX-527 transfection in high-glucose-induced Risa inhibition MPCs, but contrary to Desmin expression (Figures 4B, E). In addition, the levels of autophagy markers (Beclin-1 and LC3B) were notably downregulated, whereas the P62 level was significantly upregulated in high-glucose-induced Risa inhibition MPCs following transfection with EX-527 (Figure 4C, F). Finally, importantly, Risa inhibition transfection effectively abolished the Risa overexpression-mediated autophagy inhibition and podocyte injury by high glucose, but Sirt1 inhibition could abrogate the autophagy-promoting and anti-injury effects of Risa inhibition in high-glucose-mediated MPCs. Therefore, Risa overexpression attenuated Sirt1-mediated downstream autophagy levels and then aggravated the injury of podocytes by inhibiting the expression of Sirt1 in high glucose MPCs. Taken together, Risa suppressed autophagy and aggravated podocyte injury via the Sirt1 autophagy axis in high glucose.

## Discussion

Previous studies have demonstrated that overexpression of Risa in primary liver cells or C2C12 myotubes of mice reduces autophagy, while Risa inhibition by tail vein injection of adenovirus could enhance autophagy in ob/ob mice, thereby reducing insulin resistance [24]. Some LncRNAs, including LncRNA ZNNT1[34], SNHG8[35], LINC01116124 [36], and MEG3 [37] also have been found to be related to autophagy. However, little is known about the role and specific mechanism of Risa on DN. The major findings of this study were that Risa overexpression in high glucose acted as an adverse factor by suppressing autophagy in podocytes and thus promoted the development of DN. Risa suppressed autophagy and decreased the expression of podocytes by Sirt1 and suppression of Risa might be an effective measure in protecting the podocyte.

Autophagy is an important and complex pathophysiological mechanism of DN [38], and Sirt1 is considered as one of the most critical autophagy regulators in DN [39]. Sirt1-dependent autophagic induction in response to environmental stress is crucial for the maintenance of renal function. Sirt1, a positive regulator of autophagy, especially an important inducer of autophagic flux in the kidney, is also downregulated in diabetic kidneys [39]. In experimental models of both type 1 and type 2 diabetes, the expression and activity of Sirt1 have been reported to be reduced in the kidney [40]. Moreover, studies using Sirt1 activators in models of both type 1 and type 2 diabetes have reported renoprotective benefits [41, 42]. DN caused by hyperglycemia involves various factors, such as malnutrition or excess, energy deficiency or surplus, hypoxia, accumulation of metabolites, etc. Therefore, the pathogenesis of DN is extremely complex and the mechanisms of Sirt1 in podocyte autophagy are still lacking, but Sirt1 can deacetylate essential autophagic factors such as Atg5, Atg7, Atg8, LC3, etc., and has been shown to induce autophagy [12]. Thus, Sirt1 regulates autophagosome formation via multiple components (GSK3b, Beclin-1, P62 etc) of the autophagy machinery [43]. Although accumulating evidence has shown that GSK3 $\beta$  activity is inversely correlated with autophagy [44], the underlying mechanism has not been fully clarified. The imbalanced energy homeostasis caused by impaired glucose metabolism might lead to autophagy induction together with GSK3 $\beta$  inhibition [45]. All of these derangements acting in concert reduce the kidney's ability to maintain cellular homeostasis and health; however, the loss of Sirt1 function

seems to be particularly important [46]. Several epidemiologic studies have shown that polymorphisms in the gene encoding Sirt1 increase the risk of CKD in patients with type 2 diabetes [47]. Additionally, serum levels of Sirt1 are decreased in these patients, and this decline parallels the development of albuminuria [48].

Risa is known as a regulator of insulin sensitivity and autophagy [24]. Previous studies have demonstrated that overexpression of Risa induces insulin resistance in primary mouse hepatocytes and markedly reduces the phosphorylation level of Akt/GSK3 $\beta$ , as well as the effect of autophagy (mTOR, LC3II). Moreover, knockdown of Atg7 or Atg5 significantly inhibits the effect of knockdown of Risa on insulin resistance, suggesting that knockdown of Risa improves insulin sensitivity by enhancing autophagy and Risa is a potential target for treating insulin-resistance-related diseases [24]. Therefore, the effects of Risa overexpression and inhibition on autophagy pathway of glomerular podocytes were explored in the DN db/db mouse model and MPC. Our data showed that Risa overexpression could aggravate podocyte damage by suppressing Sirt1-mediated autophagy pathway both in db/db mice and high-glucose-treated MPCs (Figure 5). In addition, tail vein injection of Risa-AAV in DN mice or transfection with Risa-LV in high-glucose-induced MPCs could both enhance the autophagy sensitivity and podocyte level. This suggests that targeting Risa may be an effective treatment for DN. However, only a few miRNAs were found to execute their biological functions in DN via targeting Risa to date, further research is needed to explore some more biological effects and targets of Risa in glomerular podocytes as it would bring us a step closer to identifying the underlying mechanism in the pathogenesis of DN. Taken together, the data demonstrate that Risa regulates podocyte expression by affecting autophagy in DN and suggest that Risa is a potential target for treating DN.

## Conclusion

In summary, Risa was overexpressed in DN mice and high-glucose-induced MPCs. Risa overexpression decreased the Sirt1-mediated autophagy pathway and aggravated podocyte damage, and Risa inhibition could improve autophagy mediated podocyte injury. SNP r3740051 in the human Sirt1 promoter or the predicted human Risa is associated with energy expenditure when food is withheld, supporting the potential effect of the predicted human Risa on insulin sensitivity and glucose homeostasis [49]. Hence, Risa may contribute to the development of effective therapeutic agents for the treatment of human DN. Taken together, Risa regulates podocyte expression by affecting autophagy and suggests that Risa is a potential target for treating DN.

## Abbreviations

Sirt1: Sirtuin 1

DN: diabetic nephropathy

AAV: adeno-associated virus

LV: Lentivirus

qRT-PCR: quantitative real-time polymerase chain reaction

TEM: transmission electron microscope

ESRD: diabetes develops end-stage renal disease

DKD: diabetic kidney disease

UACR: urinary albumin-creatinine ratio

Scr: serum creatinine

## **Declarations**

### **Ethics approval and consent to participate**

The reasons for exemption from signing informed consent: blood, urine samples, and renal tissue samples of healthy people and blood, urine samples of diabetic nephropathy patients were taken from the biological sample bank of the First Affiliated Hospital of Zhengzhou University, and renal tissue samples of diabetic nephropathy patients were taken from the biological sample bank of the First Affiliated Hospital of Zhengzhou University. The renal tissue of patients with diabetic nephropathy came from the pathology department of the First Affiliated Hospital of Zhengzhou University. There is no risk for patients to collect renal tissue after the operation, and the right welfare of subjects is not affected by informed consent. The study was approved by the Ethics Committee of Scientific Research and Clinical Trial of the First Affiliated Hospital of Zhengzhou University (2020-KY-273).

The researchers stated that: We fully understand the ethical requirements of the ethical review measures for biomedical research involving human beings. The research group will carry out scientific research in strict accordance with the corresponding ethical principles and will not conduct research that violates medical ethics and accept the supervision and inspection of relevant ethical departments.

### **Consent for publication**

Collection of renal tissue: the normal control renal tissues were collected from the biological sample bank of the First Affiliated Hospital of Zhengzhou University (the specimens were collected from the resection of urological surgery, 3-5cm away from the edge of the lesion). The renal tissues of diabetic nephropathy were collected from the pathology department of the First Affiliated Hospital of Zhengzhou University (the samples were from the puncture tissues of diabetic nephropathy and confirmed by renal biopsy in nephrology). All patients signed informed consent before the experiment.

# Availability of data and materials

The datasets used and/or analyzed during the current study are available from the corresponding author on reasonable request.

# Competing interests

The authors declare that they have no competing interests.

# Funding

This study is supported by grants from the Joint construction project of Henan Province [No.SB201901015], General Program of the National Natural Science Foundation of China General Project [No.81970633]; the Major public welfare special projects in Henan Province [No.201300310600]; the National Natural Science Young Scientists Foundation of China [No.81800648]; Excellent Young Scientists Fund Program of the Natural Science Foundation of Henan Province [No.202300410363].

# Authors' contributions

The authors contributed equally to this work.

# Acknowledgements

Not applicable.

# References

1. Hou Y, Lin S, Qiu J, et al. NLRP3 inflammasome negatively regulates podocyte autophagy in diabetic nephropathy. *Biochem Biophys Res Commun.* 2020;521(3):791-798.
2. Dunlop M. Aldose reductase and the role of the polyol pathway in diabetic nephropathy. *Kidney Int Suppl.* 2000;77:S3-S12.
3. Miyata T, de Zeeuw D. Diabetic nephropathy: a disorder of oxygen metabolism?. *Nat Rev Nephrol.* 2010;6(2):83-95.
4. Giacco F, Brownlee M. Oxidative stress and diabetic complications. *Circ Res.* 2010;107 (9):1058-1070.
5. Cybulsky AV. Endoplasmic reticulum stress in proteinuric kidney disease. *Kidney Int.* 2010;77(3):187-193.

6. Mizushima N, Levine B, Cuervo AM, Klionsky DJ. Autophagy fights disease through cellular self-digestion. *Nature*. 2008;451(7182): 1069-1075.
7. Kroemer G, Mariño G, Levine B. Autophagy and the integrated stress response. *Mol Cell*. 2010;40(2):280-293.
8. Zeni L, Norden AGW, Cancarini G, Unwin RJ. A more tubulocentric view of diabetic kidney disease. *J Nephrol*. 2017;30(6):701-717.
9. Zhang W, Feng Y, Guo Q, et al. SIRT1 modulates cell cycle progression by regulating CHK2 acetylation-phosphorylation. *Cell Death Differ*. 2020;27(2):482-496.
10. Packer M. Autophagy-dependent and independent modulation of oxidative and organellar stress in the diabetic heart by glucose-lowering drugs. *Cardiovasc Diabetol*. 2020;19(1):62.
11. Qiu G, Li X, Wei C, et al. The Prognostic Role of SIRT1-Autophagy Axis in Gastric Cancer. *Dis Markers*. 2016;2016:6869415.
12. Lee IH, Cao L, Mostoslavsky R, et al. A role for the NAD-dependent deacetylase Sirt1 in the regulation of autophagy. *Proc Natl Acad Sci U S A*. 2008;105(9):3374-3379.
13. Yang D, Livingston MJ, Liu Z, et al. Autophagy in diabetic kidney disease: regulation, pathological role and therapeutic potential. *Cell Mol Life Sci*. 2018;75(4):669-688.
14. Wang S, Yang Y, He X, et al. Cdk5-Mediated Phosphorylation of Sirt1 Contributes to Podocyte Mitochondrial Dysfunction in Diabetic Nephropathy. *Antioxid Redox Signal*. 2021; 34(3):171-190.
15. Liu Y, Liu W, Zhang Z, et al. Yishen capsule promotes podocyte autophagy through regulating SIRT1/NF- $\kappa$ B signaling pathway to improve diabetic nephropathy. *Ren Fail*. 2021; 43(1):128-140.
16. Hong Q, Zhang L, Das B, et al. Increased podocyte Sirtuin-1 function attenuates diabetic kidney injury. *Kidney Int*. 2018;93(6):1330-1343.
17. Li J, Xing M, Zhu M, et al. Glycogen synthase kinase 3 $\beta$  induces apoptosis in cancer cells through increase of survivin nuclear localization. *Cancer Lett*. 2008;272(1):91-101.
18. Lee YJ, Han HJ. Troglitazone ameliorates high glucose-induced EMT and dysfunction of SGLTs through PI3K/Akt, GSK-3 $\beta$ , Snail1, and  $\beta$ -catenin in renal proximal tubule cells. *Am J Physiol Renal Physiol*. 2010;298(5):F1263-F1275.
19. Pal K, Cao Y, Gaisina IN, et al. Inhibition of GSK-3 induces differentiation and impaired glucose metabolism in renal cancer. *Mol Cancer Ther*. 2014;13(2):285-296.
20. Sarkar S. Regulation of autophagy by mTOR-dependent and mTOR-independent pathways: autophagy dysfunction in neurodegenerative diseases and therapeutic application of autophagy enhancers. *Biochem Soc Trans*. 2013;41(5):1103-1130.
21. Li SY, Susztak K. The long noncoding RNA Tug1 connects metabolic changes with kidney disease in podocytes. *J Clin Invest*. 2016;126(11):4072-4075.
22. Hu M, Wang R, Li X, et al. LncRNA MALAT1 is dysregulated in diabetic nephropathy and involved in high glucose-induced podocyte injury via its interplay with  $\beta$ -catenin. *J Cell Mol Med*. 2017;21(11):2732-2747.

23. Feng Y, Chen S, Xu J, et al. Dysregulation of lncRNAs GM5524 and GM15645 involved in high-glucose-induced podocyte apoptosis and autophagy in diabetic nephropathy. *Mol Med Rep.* 2018;18(4):3657-3664.
24. Wang Y, Hu Y, Sun C, et al. Down-regulation of Risa improves insulin sensitivity by enhancing autophagy. *FASEB J.* 2016;30(9):3133-3145.
25. Jin J, Shi Y, Gong J, et al. Exosome secreted from adipose-derived stem cells attenuates diabetic nephropathy by promoting autophagy flux and inhibiting apoptosis in podocyte. *Stem Cell Res Ther.* 2019;10(1):95.
26. Guo H, Wang Y, Zhang X, et al. Astragaloside IV protects against podocyte injury via SERCA2-dependent ER stress reduction and AMPK $\alpha$ -regulated autophagy induction in streptozotocin-induced diabetic nephropathy. *Sci Rep.* 2017;7(1):6852.
27. Aventaggiato M, Vernucci E, Barreca F, Russo MA, Tafani M. Sirtuins' control of autophagy and mitophagy in cancer. *Pharmacol Ther.* 2021;221:107748.
28. He C, Klionsky DJ. Regulation mechanisms and signaling pathways of autophagy. *Annu Rev Genet.* 2009;43:67-93.
29. Lee IH. Mechanisms and disease implications of sirtuin-mediated autophagic regulation. *Exp Mol Med.* 2019;51(9):1-11.
30. Dusabimana T, Kim SR, Park EJ, et al. P2Y2R contributes to the development of diabetic nephropathy by inhibiting autophagy response. *Mol Metab.* 2020;42:101089.
31. Saxena S, Mathur A, Kakkar P. Critical role of mitochondrial dysfunction and impaired mitophagy in diabetic nephropathy. *J Cell Physiol.* 2019;234(11):19223-19236.
32. Park JE, Lee H, Rho H, Hong SM, Kim SY, Lim Y. Effect of Quamoclit angulata Extract Supplementation on Oxidative Stress and Inflammation on Hyperglycemia-Induced Renal Damage in Type 2 Diabetic Mice. *Antioxidants (Basel).* 2020;9(6):459.
33. Alzahrani S, Zaitone SA, Said E, et al. Protective effect of isoliquiritigenin on experimental diabetic nephropathy in rats: Impact on Sirt-1/NF $\kappa$ B balance and NLRP3 expression. *Int Immunopharmacol.* 2020;87:106813.
34. Li P, He J, Yang Z, et al. ZNNT1 long noncoding RNA induces autophagy to inhibit tumorigenesis of uveal melanoma by regulating key autophagy gene expression. *Autophagy.* 2020;16(7):1186-1199.
35. He C, Fu Y, Chen Y, Li X. Long non-coding RNA SNHG8 promotes autophagy as a ceRNA to upregulate ATG7 by sponging microRNA-588 in colorectal cancer. *Oncol Lett.* 2021;22(2):577.
36. Beaver LM, Kuintzle R, Buchanan A, et al. Long noncoding RNAs and sulforaphane: a target for chemoprevention and suppression of prostate cancer. *J Nutr Biochem.* 2017;42:72-83.
37. Lin L, Liu X, Lv B. Long non-coding RNA MEG3 promotes autophagy and apoptosis of nasopharyngeal carcinoma cells via PTEN up-regulation by binding to microRNA-21. *J Cell Mol Med.* 2021;25(1):61-72.

38. Koch EAT, Nakhoul R, Nakhoul F, Nakhoul N. Autophagy in diabetic nephropathy: a review. *Int Urol Nephrol*. 2020;52(9):1705-1712.
39. Packer M. Role of Impaired Nutrient and Oxygen Deprivation Signaling and Deficient Autophagic Flux in Diabetic CKD Development: Implications for Understanding the Effects of Sodium-Glucose Cotransporter 2-Inhibitors. *J Am Soc Nephrol*. 2020;31(5):907-919.
40. Tikoo K, Singh K, Kabra D, Sharma V, Gaikwad A. Change in histone H3 phosphorylation, MAP kinase p38, SIR 2 and p53 expression by resveratrol in preventing streptozotocin induced type I diabetic nephropathy. *Free Radic Res*. 2008;42(4):397-404.
41. Chen KH, Hung CC, Hsu HH, Jing YH, Yang CW, Chen JK. Resveratrol ameliorates early diabetic nephropathy associated with suppression of augmented TGF- $\beta$ /smad and ERK1/2 signaling in streptozotocin-induced diabetic rats. *Chem Biol Interact*. 2011;190(1): 45-53.
42. Kitada M, Kume S, Imaizumi N, Koya D. Resveratrol improves oxidative stress and protects against diabetic nephropathy through normalization of Mn-SOD dysfunction in AMPK/SIRT1-independent pathway. *Diabetes*. 2011;60(2):634-643.
43. Kume S, Koya D. Autophagy: A Novel Therapeutic Target for Diabetic Nephropathy. *Diabetes Metab J*. 2015;39(6):451-460.
44. Zhang C, Hou B, Yu S, Chen Q, Zhang N, Li H. HGF alleviates high glucose-induced injury in podocytes by GSK3 $\beta$  inhibition and autophagy restoration. *Biochim Biophys Acta*. 2016;1863(11):2690-2699.
45. Pal K, Cao Y, Gaisina IN, et al. Inhibition of GSK-3 induces differentiation and impaired glucose metabolism in renal cancer. *Mol Cancer Ther*. 2014;13(2):285-296.
46. Mori H, Inoki K, Masutani K, et al. The mTOR pathway is highly activated in diabetic nephropathy and rapamycin has a strong therapeutic potential. *Biochem Biophys Res Commun*. 2009;384(4):471-475.
47. Zhao Y, Wei J, Hou X, et al. SIRT1 rs10823108 and FOXO1 rs17446614 responsible for genetic susceptibility to diabetic nephropathy. *Sci Rep*. 2017;7(1):10285.
48. Shao Y, Ren H, Lv C, Ma X, Wu C, Wang Q. Changes of serum Mir-217 and the correlation with the severity in type 2 diabetes patients with different stages of diabetic kidney disease. *Endocrine*. 2017;55(1):130-138.
49. Lagouge M, Argmann C, Gerhart-Hines Z, et al. Resveratrol improves mitochondrial function and protects against metabolic disease by activating SIRT1 and PGC-1 $\alpha$ . *Cell*. 2006;127(6):1109-1122.

## Figures

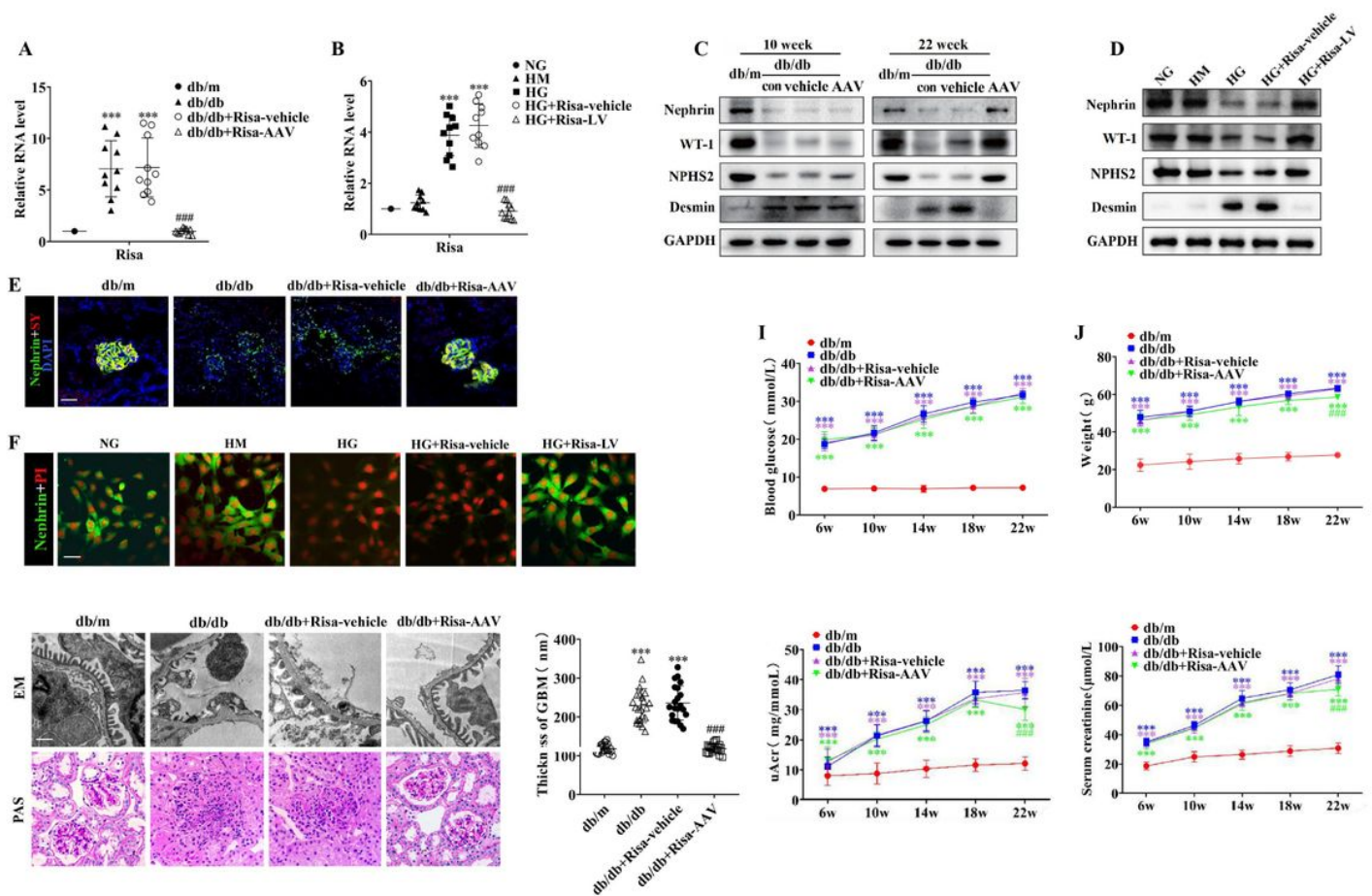


**Figure 1**

Effect of Risa overexpression and inhibition on high-glucose-induced podocyte injury. Risa expressions in DN mice (A) and MPCs (B) were examined by qRT-PCR analysis. (C) Protein levels of podocyte markers (Nephlin, WT-1, NPHS2, and Desmin) examined by western blot in DN mice transfected with Risa inhibition vector (Risa-AAV group) and empty vector in the presence of diabetes versus db/m mice, and (D) Protein levels of podocyte markers examined by western blot in MPCs transfected with Risa inhibition vector (Risa-LV group) and empty vector in the presence of high glucose versus control group. The location and expression of Nephlin in kidney tissues of mice groups (E) and MPC groups (F) were observed by confocal immunofluorescence staining. SY stands for Synaptopodin. Scale: 20  $\mu$ m. (G) The morphology of kidney and glomerular basement membrane (GBM) thickness were observed under PAS staining and TEM in mice groups. Scale bar: 20 $\mu$ m for PAS staining; 1  $\mu$ m for electron microscopy. (H) The thicknesses of GBM were calculated. Changes of random blood glucose(I), weight(J), uAcr(K), and serum creatinine(L) in mice at different time points. The data are expressed as mean  $\pm$  standard deviation from three independent experiments. \*P < 0.05, \*\*P < 0.01, \*\*\*P < 0.001 versus the healthy control group, and # P < 0.05, ## P < 0.01, ### P < 0.001 versus the experimental control group.

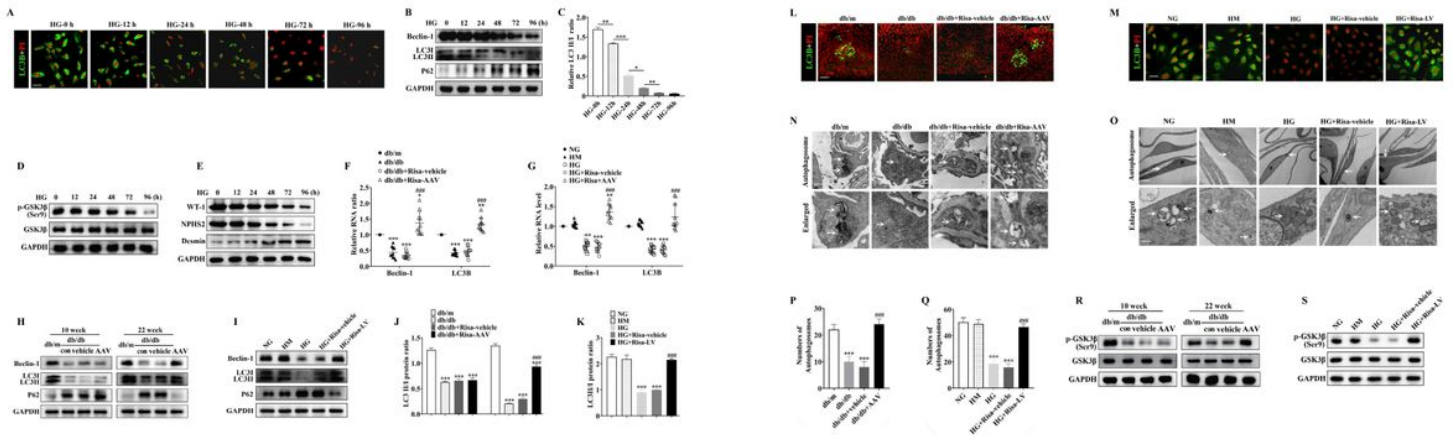


**Figure 2**

Effect of Risa Overexpression and Inhibition on High-Glucose-Induced Autophagy Damage. Autophagy expressions in MPCs were examined by immunofluorescence (LC3B) (A) and western blot (LC3B, Beclin-1 and P62) (B) in different observation time by high glucose, as well as the ratio of LC3-II/LC3-I (C). Phosphorylation of GSK3 $\beta$  (D) and podocyte markers (WT-1, NPHS2, and Desmin) (E) were observed in different observation time by high glucose. Autophagy markers (LC3B and Beclin-1) were examined by qRT-PCR in mice groups (F) and MPC groups (G). Protein levels of Beclin-1, LC3B and P62 (H,I), as well as the LC3-II/I ratio (J,K) were examined by western blot in mice groups (H,J) and MPC groups (I,K). The autophagy of podocyte was observed under TEM in mice groups (N) and MPC groups (O), as well as the numbers of autophagosomes were counted (white arrows) (P,Q). Protein levels of phosphorylated GSK3 $\beta$  were examined by western blot in mice groups (R) and MPC groups (S). Scale bar: 20 $\mu$ m for immunofluorescence. 1  $\mu$ m for autophagy electron microscopy, 200nm for enlarged autophagy. The data are expressed as mean $\pm$ standard deviation from three independent experiments. \*P < 0.05, \*\*P < 0.01, \*\*\*P < 0.001 versus the previous time group or \*P < 0.05, \*\*P < 0.01, \*\*\*P < 0.001 versus the healthy control group, and #P < 0.05, ##P < 0.01, ###P < 0.001 versus the experimental control group.

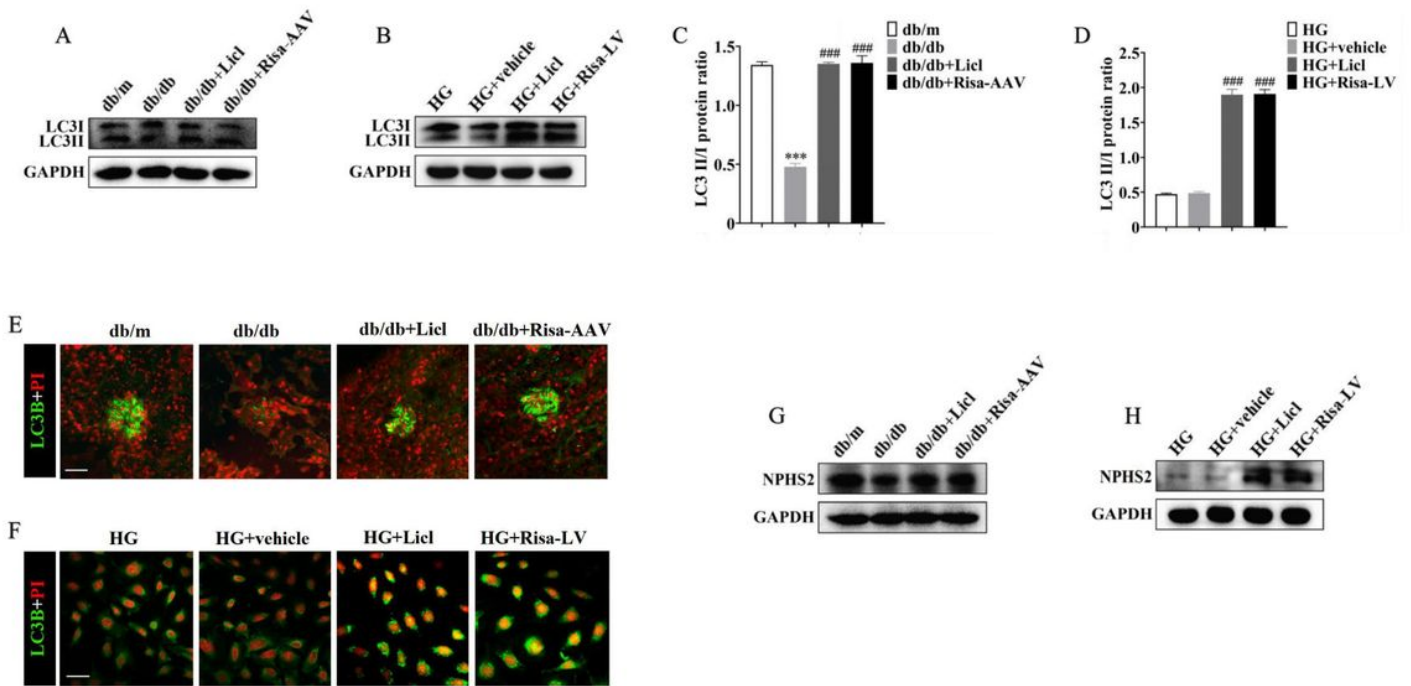


**Figure 3**

Risa overexpression exacerbated the high-glucose-induced podocyte injury by attenuating autophagy. Autophagy marker (LC3B) was examined by western blot and immunofluorescence in mice groups (A,E) and MPC groups (B,F) under Licl treatment in DN mice and high glucose MPCs, as well as the ratio of LC3II/I (C,D). NPHS2 was examined by western blot in mice groups (G) and MPC groups (H). 20 $\mu$ m for immunofluorescence. The data are expressed as mean $\pm$ standard deviation from three independent experiments. \*P < 0.05, \*\*P < 0.01, \*\*\*P < 0.001 versus the previous time group or \*P < 0.05, \*\*P < 0.01, \*\*\*P < 0.001 versus the healthy control group, and #P < 0.05, ##P < 0.01, ###P < 0.001 versus the experimental control group.

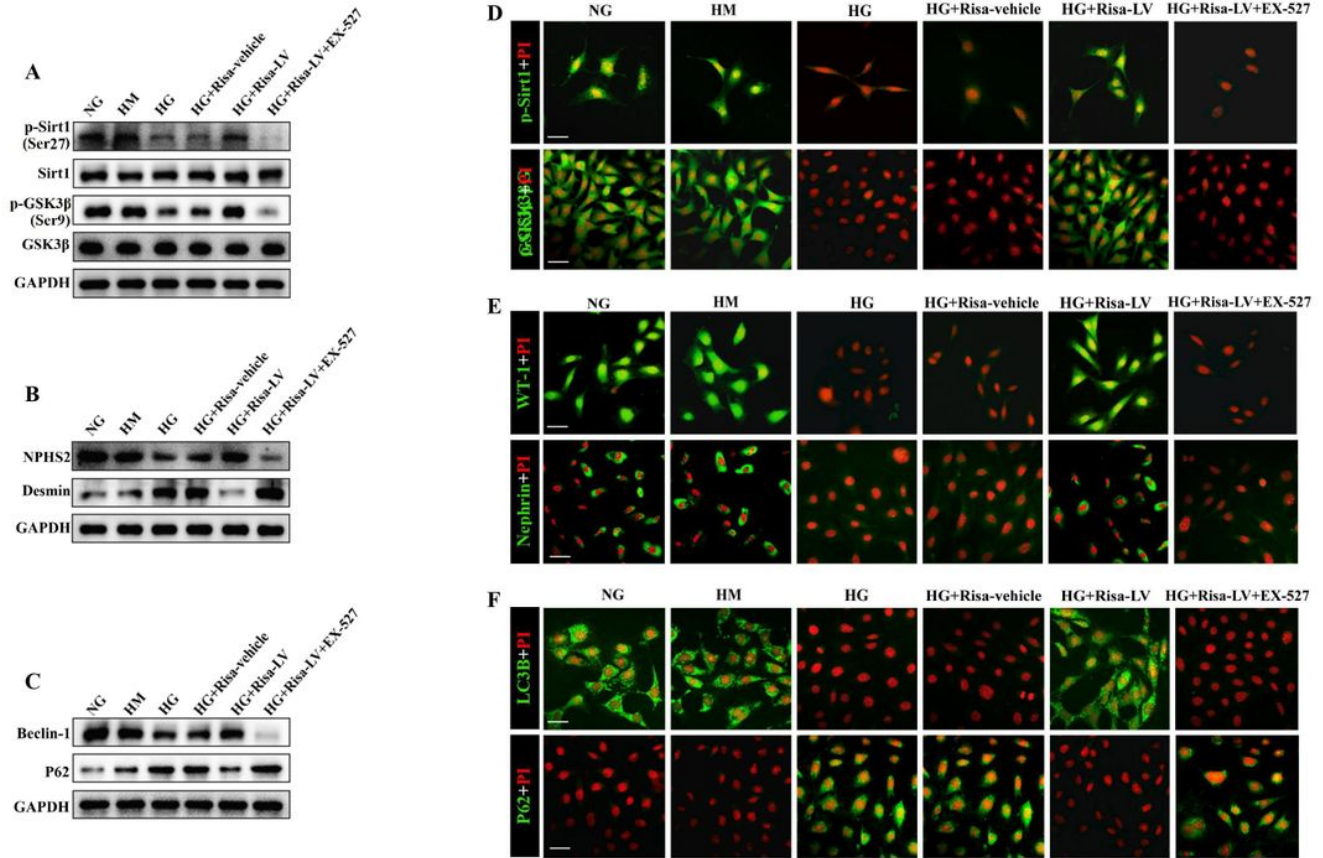


**Figure 4**

Risa Suppressed Autophagy and Aggravated Podocyte Injury Via Sirt1-mediated Autophagy Axis. Sirt1-related autophagy level examined by western blot and immunofluorescence transfected with Risa-LV vector, empty vector, and co-transfected with Risa-LV and EX-527 in high-glucose-treated podocytes compared with healthy control groups and experimental control group. Phosphorylation of Sirt1 and GSK3  $\beta$  were assessed by western blot (A) and immunofluorescence (D). Podocyte markers were assessed by western blot (NPHS2 and Desmin) (B) and immunofluorescence (WT-1 and Nephlin) (E). Expression of Beclin-1 and P62 were examined by western blot (C), as well as LC3B and P62 were assessed by immunofluorescence (F) in MPC. 20 $\mu$ m for immunofluorescence.

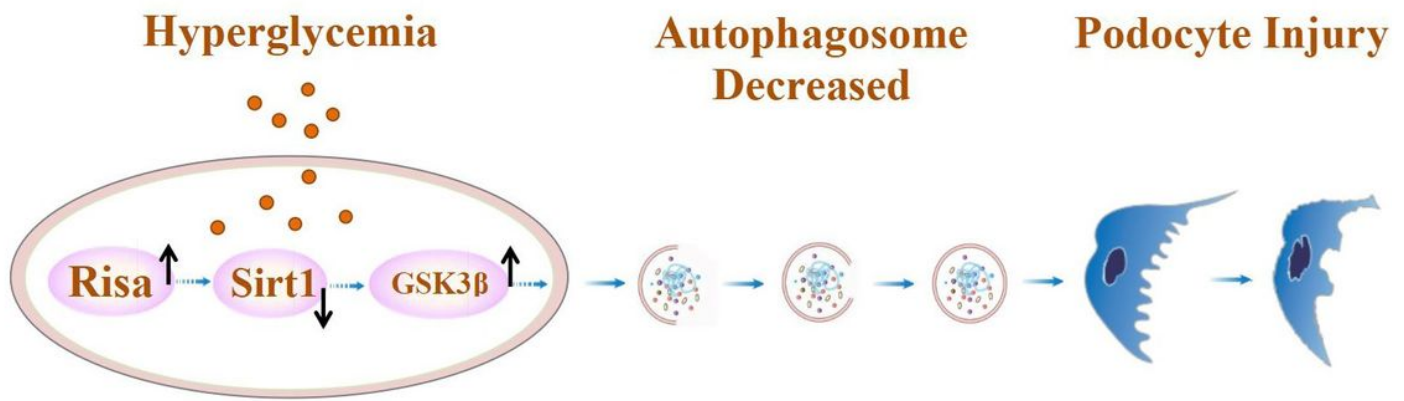


**Figure 5**

A working model for Risa regulation on podocyte injury and autophagy in DN. Under hyperglycemia, the activity and expression of Risa increased, but Sirt1 activity decreased, and activated GSK3β increased, then changed the expression and function of autophagy protein and podocyte protein through interaction and phosphorylation, which eventually led to podocyte damage.

## Supplementary Files

This is a list of supplementary files associated with this preprint. Click to download.

- [3SupplementalFigure.pdf](#)